Received: 6 December 2020 | Accepted: 10 January 2021

DOI: 10.1049/bme2.12022

IET Biometrics

The Institution of Engineering and Technology WILEY

ORIGINAL RESEARCH PAPER

Efficient high-speed framework for sparse representation-based iris recognition

Michael Melek | **Mohamed F. Abu-Elyazeed** | **Ahmed Khattab**

Electronics and Electrical Communications Engineering Department, Cairo University, Giza, Egypt

Correspondence

Michael Melek, Electronics and Electrical Communications Engineering Department, Cairo University, 12613, Giza, Egypt.
Email: michaelmelek@cu.edu.eg

Abstract

While various frameworks for iris recognition have been proposed, most lack efficiency and high speed. A new framework for iris recognition is presented that is both efficient and fast. Feature extraction is performed by extracting Gabor features and then applying supervised locality-preserving projections with heat kernel weights, which improves the recognition rate in comparison with the results from unsupervised dimensionality reduction techniques such as principal component analysis, locality-preserving projections, and random projections. Afterwards, a classification is performed using the recently proposed sparse representation-based classification (SRC). To considerably improve classification performance, SRC is proposed, using a greedy compressed-sensing recovery algorithm, as opposed to employing the traditional computationally expensive ℓ_1 minimisation. The proposed framework achieves a recognition rate of about 99.5% using two iris databases, with a significant improvement in speed over related frameworks.

1 | INTRODUCTION

Over the last 2 decades, interest in biometric personal recognition has significantly increased. The human iris is a very useful biometric feature for personal identification. Compared with other biometric features, the iris has various advantages in personal identification: it is unique, stable over the time, and does not change with age. It has a complex pattern containing many distinctive features exhibiting enormous variability among different persons [1, 2]. Consequently, iris recognition is applied in many areas including border and access control, banking, mobile authentication and national identification programs [3].

A typical iris recognition system consists of image preprocessing, feature extraction and classification. Preprocessing of the iris image targets the extraction of the location of the iris and converts the annular region of the iris from polar to rectangular coordinates. Discriminative features are then extracted from the iris. Dimensionality reduction typically follows, and is applied to remove redundancy and improve efficiency, by projecting either the iris image or the extracted features from a higher-dimensional space to a lower-dimensional subspace or submanifold. Subsequently, the iris image is classified according to some classification technique.

Various dimensionality reduction techniques have been applied in iris recognition systems. Examples include principal component analysis (PCA) [4, 5], Fisher's linear discriminant (FLD) [6], and locality-preserving projections (LPPs) [7]. PCA preserves the overall global structure of the iris image space. FLD targets preservation of the discriminating information between the images of different persons. However, both PCA and FLD fail to discover the underlying structure when iris images lie on a nonlinear submanifold hidden in the iris image space. On the other hand, LPPs target preservation of the local neighbourhood information of the image space, by projecting closer images onto closer projections. However, most iris recognition systems that employ LPPs are based on unsupervised LPP. The unsupervised version of LPP merely projects closer images onto closer projections irrespective of the classes. Consequently, the recognition rates obtained are not sufficiently high.

Dimensionality reduction techniques can be applied directly to the iris image, or more commonly, to features extracted from the iris image. Such features include discrete wavelet transform (DWT) coefficients and Gabor coefficients, with the latter being most commonly used.

The classification stage follows feature extraction. Various classification techniques have been utilised for iris recognition,

including nearest neighbour, nearest subspace, support vector machines (SVMs) and neural networks. However, a recently developed classification technique termed sparse representation-based classification (SRC) has given promising results by outperforming other traditional techniques [8, 9]. SRC is based on the theory of compressed sensing (CS) [10, 11], which targets the reconstruction of sparse data from sub-Nyquist measurements. The SRC technique is based on the assumption that a test sample can be represented as a linear combination of training samples. This results in a sparse representation because the only significant coefficients are those corresponding to the class of the test sample. Subsequently, CS recovery algorithms are utilised to obtain the sparse representation and thereby find the target class. Traditionally, ℓ_1 minimisation has been used for CS recovery and for SRC. However, it is computationally expensive and results in reconstruction delays that may not be tolerable in most real-time applications. Other greedy recovery algorithms have been proposed to reduce the computational complexity of ℓ_1 minimisation. However, most of these result in a significant loss in reconstruction accuracy, such as orthogonal matching pursuit (OMP) [12], which reduces complexity to some extent.

In this paper, we propose an efficient and fast iris recognition framework. The main contributions of this work are as follows:

- Supervised locality-preserving projections (SLPPs) with heat kernel weights are used for dimensionality reduction and applied to extracted Gabor features. Such a technique is used for manifold learning, where closer images in the iris space are mapped to closer points in the low-dimensional space and vice versa. Furthermore, using the supervised version, which accounts for the different classes, enhances classification performance. This is in contrast to other unsupervised techniques that are traditionally used, such as PCA, LPP and random projections.
- SRC is performed using our adaptive reduced-set matching pursuit (ARMP) algorithm [13]. Other frameworks that employ SRC typically perform CS reconstruction using the computationally expensive ℓ_1 minimisation such as those in [9, 14]. In contrast, ARMP is an efficient CS reconstruction algorithm that significantly improves the speed of SRC while it maintains the same accuracy.

Therefore, combining the two ideas results in an iris recognition framework that is both fast and accurate. Using simulations, we have analysed in detail the impact of each of the above two components and compared each of them with the corresponding components used in other iris recognition frameworks.

The feature extraction stage of our proposed framework proceeds as follows. Iris images are preprocessed using circular Hough transform to extract the iris region, which is then converted into rectangular coordinates. Gabor features are extracted. Then, we perform dimensionality reduction using SLPP. Such a technique significantly improves the recognition rate. In the classification stage, we utilise SRC using the ARMP algorithm. This results in a very accurate and efficient framework that is suitable for real-time applications.

The rest of this paper is organised as follows. Section 2 discusses some related works. We present the preprocessing and feature extraction stages of our proposed framework in Section 3 and the classification stage in Section 4. Experimental results are presented in Section 5. Section 6 concludes the paper.

2 | RELATED WORK

Various iris recognition systems have been developed over the past few decades. The vast majority employ dimensionality reduction techniques. For example, an iris recognition system based on PCA is developed in [15]. Then, a nearest neighbour classifier is used for classification. Linear discriminant analysis (LDA) is employed in [16] and is applied to DWT coefficients extracted from the iris image. This is followed by a probabilistic neural network classifier. Two-dimensional versions of the aforementioned techniques (2D-PCA and 2D-LDA) are utilised in [17]. Classification is performed using a nearest neighbour classifier. Independent component analysis is used in [18] followed by a nearest neighbour classifier.

Other works employ LPPs for dimensionality reduction. For instance, [19] utilised LPP to perform manifold learning. Subsequently, an SVM classifier is utilised to find and establish the optimal classification hyperplane in low-dimensional space. Moreover, [20] combined LPP with random permutations to generate an encrypted biometric template. Then, nearest neighbour classification was performed. However, both works utilise the unsupervised version of LPP, which does not account for class information.

While dimensionality reduction techniques can be applied directly to image pixels, other works apply such techniques to features extracted from the iris images. For example, [21] applies DWT to a histogram-equalised iris image. Then, the extracted DWT coefficients are input into the PCA algorithm for dimensionality reduction. Subsequently, K-nearest neighbours (KNN), random forest, and SVM classifiers are utilised and compared. Alternatively, many works extract Gabor features from iris images and then apply dimensionality reduction techniques to the extracted features. For instance, [19] applies LPP to extracted Gabor features at five scales and eight orientations.

Some works introduce other features for use in iris recognition. For example, [22] uses a combination of scattering and textural features. Scattering features provide rich descriptors for complex structures because they retain high-frequency information. Dimensionality reduction using PCA is applied to the extracted features and a minimum distance classifier utilised.

As the theory of CS found application in many fields, a novel classification technique based on it was developed by Wright et al. [8]. This technique was termed sparse representation-based classification and was applied successfully to face recognition [8, 23]. Based on SRC, an iris recognition system was developed in [9]. Gabor features are extracted and dimensionality reduction is performed through random projections. The iris image is then divided into different sectors that are recognized separately using SRC. The results of

different sectors are combined based on quality through a Bayesian fusion framework. Random projections have the benefit of enhanced privacy and security. Another system based on SRC is developed in [14]. Again, the iris image is divided into sectors and SRC is applied to each sector. Three classifiers are then utilised: KNN, sector-based classifier and cumulative sparse concentration index. A genetic algorithm is then used to learn the weight of each classifier. However, both of the aforementioned works utilise ℓ_1 minimisation for CS recovery during SRC. Such a technique is computationally expensive and limits recognition speed.

Over the past few years, with progress in deep learning, deep convolutional neural networks have been utilised for iris recognition systems [24]. Such systems do not need hand-crafted features, because they utilise a convolutional neural network (CNN) to learn the features. However, a massive amount of training data, training time, memory, storage, and processing power is required to obtain acceptable results. A deep learning–based method termed DeepIrisNet is proposed in [25]. It integrates the most popular components from more recent successful CNNs, such as dropout learning, small filter size, very deep architecture, rectified linear non-linearity, and batch normalisation. On the other hand, [26] explores the performance of state-of-the-art pretrained CNNs on iris recognition. A deep learning method based on capsule network architecture is proposed in [27]. Such a network increases the robustness of the model.

In [28], a pretrained AlexNet CNN is utilised for feature extraction. The output of the first fully connected layer is then used for the features, which are input into a multi-class SVM algorithm to perform classification. In [29], a VGGNet CNN is utilised for feature extraction. PCA is used for dimensionality reduction followed by an SVM classifier. In [30], a pretrained ResNet of 50 layers is used for learning features and classification. In [31], a pretrained ResNet18 is used in which the last fully connected layer is replaced with a layer that has the required number of output classes.

Furthermore, deep learning has been used for iris segmentation and recognition. For example, [32] proposes a two-stage iris segmentation scheme based on CNN that is capable of accurate segmentation in noisy environments by visible light camera sensor. The first stage includes filtering, noise removal, Canny edge detector, contrast enhancement, and modified Hough transform to segment and approximate the iris boundary. The second stage includes a deep CNN to fit the true iris boundary.

3 | PREPROCESSING AND PROPOSED FEATURE EXTRACTION

In this paper, we propose a fast and efficient framework for iris recognition. In this section, we describe the preprocessing and feature extraction stages of our proposed framework. First, we locate the iris region and convert it into rectangular coordinates. Then, we extract Gabor features from iris images and augment the resulting features into a column vector. Finally, we apply SLPPs using heat kernel weights to the resulting vectors. Our proposed approach achieves higher recognition rates than other approaches that employ other dimensionality reduction techniques.

3.1 | Preprocessing

Preprocessing targets the extraction of the iris region from the eye image and its conversion into a form suitable for further processing. Iris images are preprocessed using circular Hough transform [33] to find the inner and outer boundaries of the iris. Consequently, the iris region is located. Then, the iris region is converted from polar to rectangular coordinates using Daugman's rubber sheet model [1]. This is more convenient for subsequent stages.

3.2 | Gabor features

Gabor wavelets are widely used to extract local features for pattern recognition [34]. This is due to their ability to provide optimised resolution in both spatial and frequency domains [35, 36]. After preprocessing, we use Gabor wavelets of five scales and eight orientations [37]. Gabor features are extracted by taking the magnitudes of the two-dimensional convolution of the iris images with the family of Gabor wavelets. Extracted features are then downsampled. They are then normalized to zero mean and unit variance. The resultant features are then converted into a single column vector representing the input image.

3.3 | Supervised locality-preserving projections

We then apply dimensionality reduction to the extracted Gabor features. This reduces computational complexity and improves the recognition rate [38]. Some works suggest the application of any dimensionality reduction technique, even very simple random projections [8, 9]. They argue that such a technique eventually achieves a high recognition rate when the number of features extracts becomes sufficiently high. However, we suggest that employing a dimensionality reduction technique that requires the least number of features for a given recognition rate results in the best performance. This is because using fewer features results in faster recognition and therefore improves algorithm speed. This will be demonstrated using simulations.

3.3.1 | Manifold learning

In contrast to PCA, which targets preservation of the global structure of the iris space, manifold learning techniques target preservation of the local structure of the iris space [39]. This means that closer points in the higher-dimensional iris space

are mapped to closer points in the low-dimensional space and vice versa.

Our framework uses SLPPs for manifold learning. In contrast to other algorithms that are based on unsupervised LPP, we propose using supervised LPP, which performs dimensionality reduction while accounting for the classes of the samples.

The manifold structure is modelled by an adjacency graph that captures the local structure of the iris space [39]. Each training sample is represented by a node. In unsupervised LPP, a nearest neighbour graph is formed in which two nodes are connected if either one lies in the k nearest neighbours of the other. In contrast, the adjacency graph used in supervised LPP takes the classes into account. This is accomplished by connecting any two nodes if they belong to the same class. This results in a projection with improved classification ability. Moreover, the weights of the graph that we form are the heat kernels, which improve the learning process and accordingly improve the recognition rate. The weight of the edge connecting nodes x_i and x_j is $e^{-\|x_i-x_j\|^2/t}$ [40], where $t \in \mathbb{R}$ determines the rate of decay. Thus, the graph weights are given by

$$S_{ij} = \begin{cases} e^{-\|x_i-x_j\|^2/t}, & \text{if } x_i \text{ and } x_j \text{ belongtothesameclass} \\ 0, & \text{otherwise} \end{cases} \tag{1}$$

Subsequently, we proceed as in the Laplacianfaces algorithm [39].

4 | ADAPTIVE REDUCED-SET MATCHING PURSUIT-BASED CLASSIFICATION

In this section, we present the classification stage of our proposed framework. We use the SRC algorithm proposed in [8]. However, rather than using ℓ_1 minimisation for CS recovery, we use our ARMP algorithm. This results in a significant improvement in speed with a very high recognition rate. SRC is based on the theory of CS. We first review the theory of CS and then describe SRC. Finally, we show how we use ARMP for classification.

4.1 | Compressed sensing review

Consider a sparse signal, $x \in \mathbb{R}^n$, of sparsity k. A measurement system that acquires $m \ll n$ linear measurements is represented as

$$y = \Phi x, \tag{2}$$

where $\Phi \in \mathbb{R}^{m \times n}$ is the sensing or measurement matrix, and $y \in \mathbb{R}^m$ is the measured vector or the samples. The original signal x can be reconstructed from measurement vector y, given that the sensing matrix satisfies the restricted isometry property [41]. Such a condition is satisfied with high probability by matrices of entries that are independent and identically distributed and follow a Gaussian, Bernoulli or sub-Gaussian distribution. ℓ_1 minimisation was originally suggested for reconstructing the sparse signal as follows [11]:

$$\hat{x} = \arg\min_z \|z\|_1 \text{ subject to } y = \Phi z \tag{3}$$

4.2 | Sparse representation-based classification overview

Based on CS theory, SRC has been proposed [8]. Such a classification technique is found to outperform other traditional classifiers such as nearest neighbour in terms of recognition rate. Here, we review the SRC algorithm (Algorithm 1).

Consider a set of training samples belonging to n subjects. Consider a test sample y. Classifying the test sample is required, assuming that it can be approximated as a linear combination of some or all of the training samples from the corresponding class. Now let matrix A_i contain columns that are the training samples of class i. Now, form augmented matrix A as

$$A = [A_1, A_2, \ldots, A_n] \tag{4}$$

Assume that vector x contains the weights required to approximate test sample y as a linear combination of the training samples. Therefore, y can be expressed as

$$y = Ax = [A_1, A_2, \ldots, A_n]x \tag{5}$$

The elements of larger magnitude in vector x are at indices corresponding to the class of the test sample. Other elements are of negligible value. Consequently, vector x is sparse and can be obtained using CS recovery techniques. Figure 1 illustrates such a representation. Denote the reconstructed vector by $\hat{x}$; y

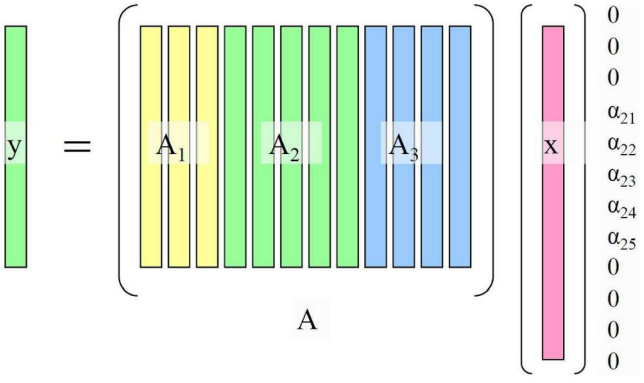

FIGURE 1 Sparse representation-based classification [8]

is then reconstructed from linear combinations of the columns of A using elements of $\hat{x}$ associated with each subject individually. Subsequently, the test sample is classified as belonging to the subject that corresponds to the least reconstruction error.

Algorithm 1 Sparse Representation-Based Classification

Input: A matrix of training samples $A = [A_1, A_2, \ldots, A_{nc}] \in \mathbb{R}^{k \times n}$ for nc classes, a test sample $y \in \mathbb{R}^k$.
1. Normalise the columns of A to have unit ℓ_2-norm.
2. Solve $y = Ax$ using ARMP (given in the following section).
3. Compute the residuals $r_i(y) = \|y - A\delta_i(\hat{x})\|_2$ for $i = 1, \ldots, nc$, where $\delta_i(\hat{x})$ is a new vector whose only nonzero entries are the entries in $\hat{x}$ corresponding to class i.
Output: Identity. $(y) = \arg\min_i r_i(y)$

4.3 | Proposed adaptive reduced-set matching pursuit

ARMP is a fast and accurate greedy recovery algorithm for CS [13]. It iteratively recovers a sparse signal x from a few sub-Nyquist measurements y. To do so, it identifies the support of the sparse signal x (its nonzero indices) by correlating y with the columns of the sensing matrix Φ. To use ARMP for SRC, the sensing matrix Φ will be taken as the matrix A given by (4). In each iteration, ARMP identifies an estimate of the support of the sparse signal. This is performed by adaptively selecting the top-magnitude elements from a reduced set of the correlation values. The sparse signal is then estimated based on the estimated support by least square minimisation. Subsequently, ARMP excludes the incorrectly selected elements, a process referred to as pruning. Then, a residual is calculated and the aforementioned steps are repeated until a stopping condition is satisfied. The components of ARMP are explained in the following.

4.3.1 | Support identification

The vector y is correlated with the columns of the sensing matrix Φ. Then, a group of the top-magnitude correlation values is selected based on a double-thresholding technique. First, a reduced set containing the top-magnitude $\beta.k$ correlation values is formed. Then, elements of magnitude larger than fraction α of the top-magnitude element are selected, and their indices are merged with the already identified support set.

The choice of α and β is discussed in [42]. The utilization of the two thresholds targets the selection of an optimum number of elements per iteration. We have shown, using exhaustive simulation, that moderate values of $\alpha \in [0.5, 0.7]$ and $\beta \in [0.15, 0.75]$ achieve the best performance because they result in a number of selected elements per iteration that is neither too large nor too small. Furthermore, the simulation results indicate that the reconstruction accuracy and speed of the algorithm are not sensitive to the particular values of α and β as long as they are in the previously mentioned optimum range.

4.3.2 | Signal estimation

The second stage of the algorithm involves estimation of the sparse signal based on the identified support set from the previous stage. A signal estimate $\hat{x}$ is obtained using least square minimisation, where we find the signal $\hat{x}$ that minimises $\|y - \Phi\hat{x}\|_2$. Such minimisation is performed by multiplication by the pseudo-inverse given by

$$\Phi_T^{\dagger} = (\Phi_T^T \Phi_T)^{-1} \Phi_T^T, \tag{6}$$

where Φ_T is a matrix containing the columns of Φ at indices from the identified support set T. We note here that calculation of the pseudo-inverse involves the inversion of a matrix of dimension equal to the number of indices in the identified support set. Because ARMP targets the selection of an optimum number of elements per iteration, much smaller than that selected by other related algorithms, the size of the matrix Φ_T is smaller, and reconstruction is faster. Furthermore, the sparsity of $\hat{x}$ is approximately equal to the number of training samples per class, which is typically small. Therefore, this operation is quite fast.

4.3.3 | Pruning

The estimated signal is refined, or pruned, by excluding incorrectly selected elements. This is done by retaining only the top k magnitude components of the estimated signal and setting the rest to zero. In other words, the support set is refined by excluding elements that account for the least contributions to the estimated signal. The rationale behind pruning is that during support identification, one or more elements of indices that do not belong to the support set of the original target signal are inevitably selected. Pruning aims to remove such incorrectly selected elements, which improves reconstruction accuracy and speed. Otherwise, such elements would remain in the signal estimate during subsequent iterations, resulting in estimation of a signal of incorrect support and in turn reducing the recognition rate when applying SRC.

4.3.4 | Residual calculation

ARMP then calculates a residual by subtracting the contribution of the pruned estimated signal from y. The residual is given by:

$$r = y - \Phi\hat{x} \tag{7}$$

This allows us to keep pursuing the remaining part of the signal x that is not yet estimated. ARMP then correlates the residual with the columns of the sensing matrix. The aforementioned steps are repeated until a stopping criterion is satisfied. ARMP terminates if the size of the residual becomes sufficiently small or if the change in the size of the residual in two successive iterations becomes sufficiently small, whichever occurs first. Otherwise, a maximum of k iterations are performed.

We summarise the proposed algorithm in Algorithm 2. The operator $L_k(\cdot)$ returns the indices of the k largest magnitudes of its argument. The hard thresholding operator $H_k(\cdot)$ retains only the k largest magnitude elements and sets the rest to zero.

Algorithm 2 Adaptive Reduced-Set Matching Pursuit

Input: Sensing matrix Φ (matrix that contains the training samples), measurement vector y (sample to be classified), sparsity level k (number of samples per class), parameters α and β.
Initialise: $\hat{x}^{[0]} = 0, r^{[0]} = y, T^{[0]} = \varnothing$.
for $i = 1$; $i := i + 1$ until the stopping criterion is satisfied do
$g^{[i]} \leftarrow \Phi^* r^{[i-1]}$ {Form correlation vector}
$J \leftarrow L_{\beta k}(g^{[i]})$ {Indices of βk elements of largest magnitude in g}
$W \leftarrow \{j : |g_j^{[i]}| \geq \alpha \max_l |g_l^{[i]}|, j \in J\}$ {Indices of elements in J of larger magnitude than the threshold}
$T \leftarrow W \cup \text{supp}(\hat{x}^{[i-1]})$ {Support merging}
$b|_T \leftarrow \Phi_T^{\dagger} y$, $b|_{T^c} \leftarrow 0$ {Signal estimation}
$\hat{x}^{[i]} \leftarrow H_k(b)$ {Pruning}
$r \leftarrow y - \Phi\hat{x}^{[i]}$ {Residual update}
end for
Output: Reconstructed signal $\hat{x}$

4.3.5 | Extending the algorithm to perform authentication

While SRC is typically used for recognition, it can be modified to perform authentication as well. In this problem, some of the test samples to be classified do not belong to the training set, and we are required to determine which ones do not belong.

In SRC, when the test sample belongs to one of the training classes, the reconstruction error for the correct class is much smaller than for the others. However, if the test sample does not belong to any of the training classes, none of the classes exhibit significantly less error than the others. Therefore, a simple comparison between the minimum error and next minimum value is a very powerful indicator as to whether the test sample belongs to the training set.

More specifically, the difference between the smallest error and the next smallest is compared with a threshold. If the difference is larger than a threshold, say 20% of the maximum error value, we deduce that the test sample belongs to the training set and is classified as belonging to the class with the minimum error. Otherwise, we deduce that the test sample does not belong to the training set.

5 | EXPERIMENTAL RESULTS

We first introduce the databases that we use to evaluate our proposed framework. Then, we describe the simulation setup. Finally, we present the simulation results.

5.1 | Databases used

5.1.1 | CASIA database

The CASIA Iris Image version 1.0 database (CASIA-IrisV1) [43] includes 756 iris images from 108 eyes. For each eye, seven images are captured in two sessions. All images have a resolution of 320 × 280.

5.1.2 | IIT Delhi Iris database

The IIT Delhi Iris database [44] consists of the iris images of 224 persons. For each person, five iris images are available. The resolution of the images is 320 × 240. We use the normalized version consisting of 1120 images for the 224 persons and with five images per person.

5.2 | Simulation setup

We use a cross-validation scheme [45] to evaluate performance. All experiments are repeated for five iterations. In each iteration, we randomly select four iris images for training and use the rest for testing. The results presented are the average of the five iterations. We use Gabor wavelets of five scales and eight orientations [37]. The features are then downsampled by a factor $\rho = 64$. Dimensionality reduction is applied to the downsampled features, and then classification is performed using the SRC algorithm. For the ARMP algorithm, we take $\alpha = 0.7$ and $\beta = 0.2$. The interested reader is referred to [42], although as explained therein, the accuracy of the algorithm is not sensitive to the exact values of α and β.

5.3 | Simulation results

In this section, we present detailed simulation results. Our proposed algorithm has two main contributions: (i) dimensionality reduction using SLPP with heat kernels and (ii) ARMP for SRC. First, we compare the performance of our

proposed framework against the performance of related frameworks. Then, to evaluate the benefit of each component of our framework, we fix other stages of the framework and compare the performance of the particular component with the corresponding components in the related frameworks. Thus, we perform three experiments. First, we test different dimensionality reduction techniques while performing classification using ARMP-based SRC. Then, we test different classifiers, fixing the SLPP technique. Finally, we fix SLPP and test SRC using ℓ_1 minimisation and ARMP. We then compare our framework with frameworks based on other features including deep learning. Finally, we evaluate the performance of our algorithm for authentication, that is, when some test samples do not belong to the training samples.

5.3.1 | Comparison with related algorithms

To evaluate the contribution of our proposed algorithm, we compare it with related algorithms. One of these utilises unsupervised LPP [19], and the other utilises SRC [9]. In [9], Gabor features are extracted from the iris region. Dimensionality reduction is performed using random projections. Then, sector-based SRC is performed, where each iris image is divided into different sectors and each is recognized separately using SRC. The results of different sectors are combined based on their quality through a Bayesian fusion framework. Random projections have the benefit of enhanced privacy and security. However, because ℓ_1 minimisation is utilised for CS recovery, reconstruction speed is limited.

In [19], Gabor features are extracted from iris regions. Dimensionality reduction is performed using unsupervised LPP. Classification is then performed using an SVM classifier.

In our proposed framework, we extract Gabor features and then apply SLPP for dimensionality reduction. For classification, we apply SRC and use ARMP for CS recovery.

Figures 2 and 3 depict the recognition rate and time, respectively, for the CASIA database. As expected, increasing the number of features improves the recognition rate to a certain extent, while recognition time generally increases. Our algorithm (SLPP + SRC) gives the highest recognition rate, of about 99.5% at 100 features, while taking the lowest time of about 5 ms. Unsupervised LPP with SVM (LPP + SVM) [19] gives a significantly lower recognition rate, 84.2% at 120 features, while taking 30 ms. Finally, the random projections with sector-based SRC (Rand + SSRC) [9] method gives a reconstruction rate of 93% at 120 features while taking 410 ms.

Combining the accurate manifold learning by supervised LPP and the accurate and efficient ARMP-based SRC, our proposed algorithm outperforms the two related algorithms in terms of both accuracy and speed. The recognition rate of unsupervised LPP is significantly less because it ignores information about the classes. On the other hand, in attempting to alleviate the computational complexity of ℓ_1 minimisation, the algorithm of [9] uses sector-based SRC, which partially reduces the reconstruction time at the expense of a reduced recognition rate.

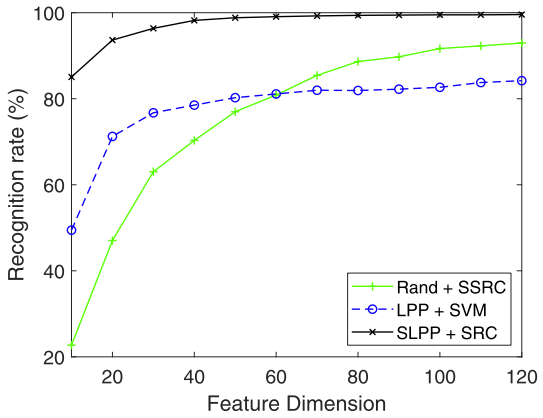

FIGURE 2 Recognition rate for the CASIA database

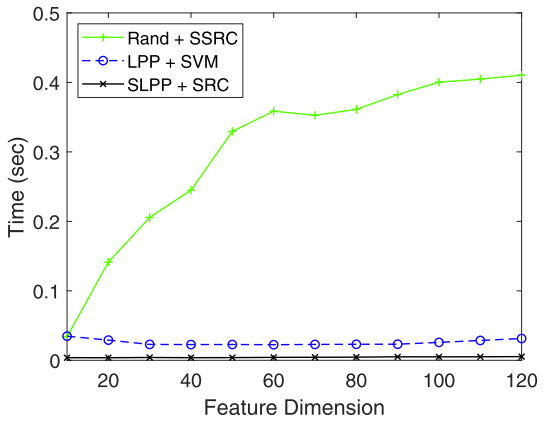

FIGURE 3 Recognition time for the CASIA database

Figures 4 and 5 depict the recognition rate and time, respectively, for the IIT Delhi database. Again, our proposed algorithm shows superior performance in terms of accuracy and speed compared with the other two algorithms. We obtain a recognition rate of 99.6% at 30 features in 5 ms. LPP + SVM gives a recognition rate of 97.6% at 60 features in 49 ms, while the random projections with sector-based SRC (Rand + SSRC) [9] method gives a reconstruction rate of 97.6% at 50 features in 363 ms.

5.3.2 | Comparison of dimensionality reduction techniques

In the following experiment, we compare the performance of different dimensionality reduction techniques. To perform a fair comparison, we fix the other stages of the algorithm, we perform the following classification using ARMP-based SRC. Figure 6 depicts the recognition rate using different dimensionality reduction techniques that are applied to Gabor features extracted from the images. SLPP gives the highest recognition rate of 99.5% using 100 features. Next comes LPP at 97.2% and 120 features, followed by random projections at 90.3% and 120 features. This shows the benefit of SLPP in

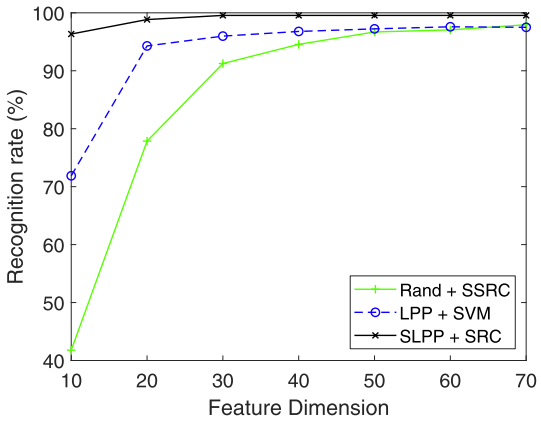

FIGURE 4 Recognition rate for the IIT Delhi database. LPP, locality preserving projections; SLPP, supervised locality preserving projection; SRC, sparse representation-based classification; SVM, support vector machine

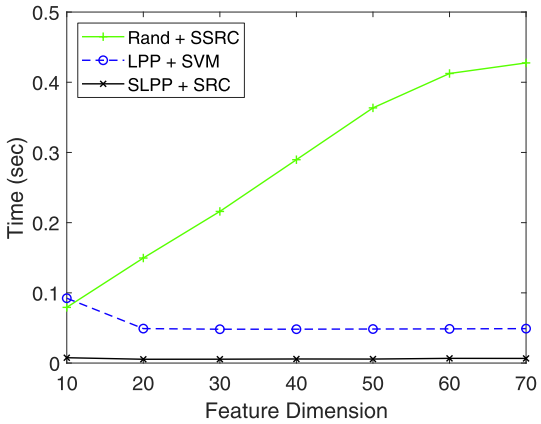

FIGURE 5 Recognition time for the IIT Delhi database. LPP, locality preserving projections; SLPP, supervised locality preserving projection; SRC, sparse representation-based classification; SVM, support vector machine

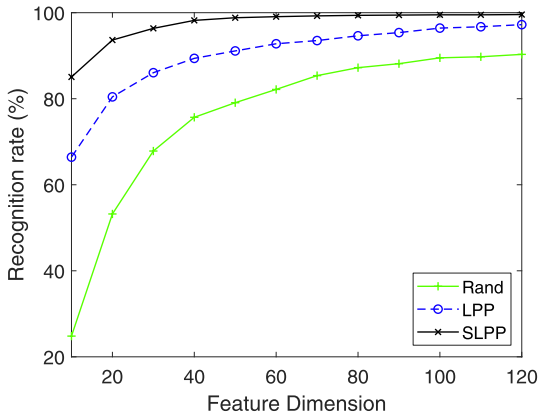

FIGURE 6 Recognition rate using different dimensionality reduction techniques. LPP, locality preserving projections; SLPP, supervised locality preserving projection

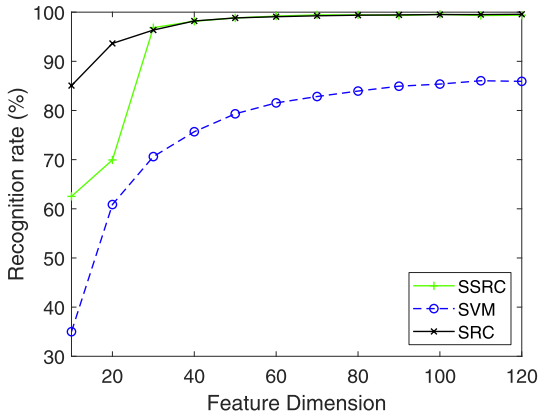

FIGURE 7 Recognition rate using different classifiers. SLPP, supervised locality preserving projection; SRC, sparse representation-based classification; SVM, support vector machine

efficient manifold learning, as opposed to the two unsupervised techniques that do not take class information into account. Different dimensionality reduction techniques do not have a significant impact on reconstruction time, and therefore we do not show the reconstruction time graph for this experiment.

5.3.3 | Comparison of different classifiers

In the following experiment, we demonstrate the benefit of using SRC over other classifiers (sector-based SRC and SVM) while fixing the SLPP dimensionality reduction technique. Figures 7 and 8 illustrate the recognition rate and time, respectively, for different classifiers using the CASIA database. At lower feature dimensions, SRC gives higher recognition rates. At feature dimensions of 30 and higher, SRC and SSRC are very close at about 99.5% and 100 features. However, SRC is significantly faster, at 5 ms, as opposed to 0.4 s for sector-based SRC. This is because CS reconstruction is performed only once for the whole iris image rather than for each sector separately. On the other hand, SVM only gives a recognition rate of 85.9%. This shows the benefit of using SRC compared with other classifiers, as it achieves very high classification accuracy and speed.

5.3.4 | Comparison of compressed sensing recovery techniques used for sparse representation-based classification

Finally, we fix the dimensionality reduction part using SLPP and perform classification using SRC; however, we test our ARMP algorithm against ℓ_1 minimisation for SRC. Figures 9 and 10 show the recognition rates and times, respectively, for such experiments. At 30 and higher features, both algorithms result in a high and close reconstruction rate of 99.5% at 100 features. However, the benefit of ARMP becomes obvious when the reconstruction time is compared. ℓ_1 minimisation takes about 80 ms, while ARMP takes about 5 ms, or an

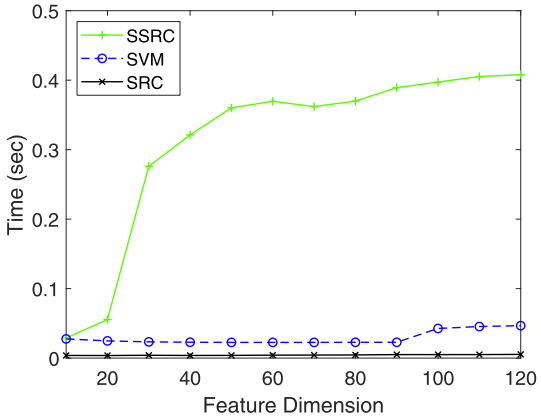

FIGURE 8 Recognition time using different classifiers. SLPP, supervised locality preserving projection; SRC, sparse representation-based classification; SVM, support vector machine

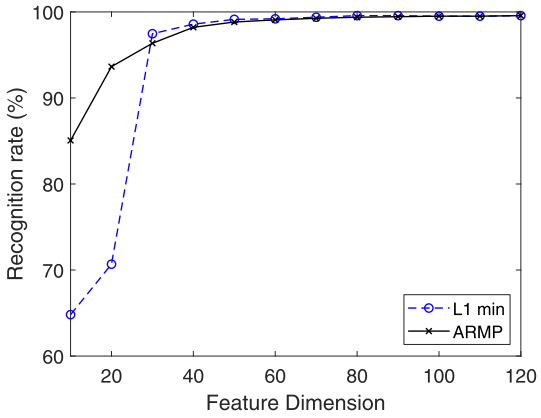

FIGURE 9 Recognition rate using different compressed sensing recovery algorithms. ARMP, adaptive reduced-set matching pursuit

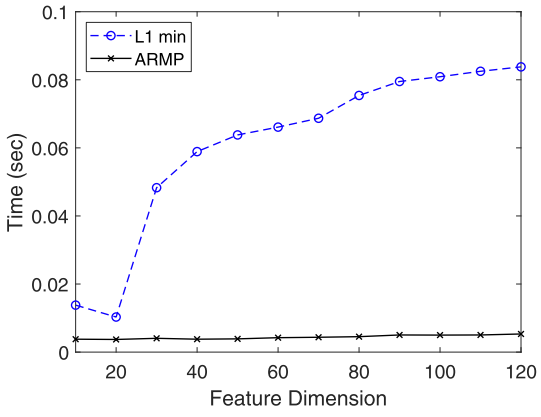

FIGURE 10 Recognition time using different compressed sensing recovery algorithms. ARMP, adaptive reduced-set matching pursuit

improvement of more than an order of magnitude in reconstruction speed. Therefore, ARMP significantly reduces the computational complexity of ℓ_1 minimisation without affecting reconstruction accuracy. Furthermore, the speed-up that results from applying ARMP as opposed to ℓ_1 minimisation renders sector division for sector-based SRC unnecessary.

TABLE 1 Comparison of frameworks based on features and deep learning

Method	Recognition rate (%)
Scattering transform and textural features [22]	99.2
AlexNet [28]	98.33
VGGNet [29]	99.4
DeepIris [30]	95.5
Our proposed framework	99.6

5.3.5 | Comparison with frameworks based on other features and deep learning

In this section, we compare the performance of our proposed framework against frameworks based on other feature extraction techniques and deep learning. First, we compare our framework with that proposed in [22], which uses a combination of scattering and textural features, followed by dimensionality reduction using PCA and a minimum distance classifier. Next, we compare our framework with three recent deep learning–based frameworks. Such frameworks do not need handcrafted features because they utilise CNNs to learn features. The first of these is based on a pretrained AlexNet CNN, followed by a multi-class SVM classifier [28]. The second is based on a VGGNet CNN [29]. PCA is then used for dimensionality reduction followed by an SVM classifier. The third uses a pretrained ResNet of 50 layers [30]. Table 1 shows a comparison of the recognition rates obtained by our proposed framework and those obtained by other frameworks using the IIT Delhi database.

In [22], 99.2% accuracy is achieved. PCA does not capture the underlying structure of the iris image space when they lie on a nonlinear submanifold hidden in the iris image space. Furthermore, it is an unsupervised technique. On the other hand, SLPP is a supervised manifold learning technique that is better suited for classification problems, especially when images lie on a nonlinear submanifold. Furthermore, the minimum distance classifier is not as accurate as SRC [8], which agrees with our simulations.

In [28], the AlexNet framework achieves 98.33% accuracy. This value is reported after normalisation of the iris images using the rubber sheet model. While higher values are reported without normalisation, they are based on using the whole segmented square region of the eye containing the iris and the pupil as inputs to the neural network. This results in an unfair comparison with methods based on merely comparing the iris region.

The accuracy of frameworks based on VGGNet and DeepIris [29, 30] shows some improvement compared with [28]; however, the accuracy is still limited compared with our

TABLE 2 Authentication accuracy

Training samples	Accuracy (%)
4	96.67
5	100
6	100

proposed framework with 99.6% accuracy. Such deep learning–based techniques require a huge amount of training data, training time, memory, storage, and processing power to obtain acceptable results.

Compared with deep learning–based frameworks, our proposed work requires less training data, training time, complexity, processing power, storage, and memory. Furthermore, our work achieves a higher recognition rate.

5.4 | Recognition and authentication

In this section, we perform an experiment to evaluate the performance of our proposed work for authentication as well as recognition. In this experiment, it is not known a priori whether the test sample belongs to the training classes. We will first perform authentication to determine whether it belongs to the training classes. If it is authenticated, recognition will be performed. In this experiment, we will use a subset of the CASIA-V1 database containing 90 training classes. For testing, we will use iris images from 10 classes that belong to the training classes and 10 classes that do not. We will perform SLPP using 100 features. SRC is performed as described in Section 4.3.5. The experiment is repeated five times, and the reported accuracy is the mean of the five trials. We repeat the experiment using four, five, and six training images per class. The accuracy reported represents correct authentication and correct recognition if the test sample is authenticated. That is, incorrect authentication or recognition reduces the accuracy. Table 2 lists the results of this experiment.

6 | CONCLUSIONS

In this paper, we have proposed a CS-based framework for iris recognition that is both fast and efficient. For feature extraction, we proposed extracting Gabor features and then applying SLPPs with heat kernel weights. This provides very efficient class-based manifold learning compared with other dimensionality reduction techniques. For classification, we proposed using ARMP for SRC. This significantly improves the speed and efficiency of our framework compared with that of related algorithms. A recognition rate of about 99.5% is achieved using two benchmark iris databases, and at faster reconstruction times than those of related algorithms. We assessed the contribution of each component of our proposed framework by comparing its performance to the similar components of other frameworks. Among different dimensionality reduction techniques, SLPP with heat kernel gives the highest recognition rate. Combining the power of SRC with the speed and efficiency of ARMP proves to be a faster and more efficient classifier than other classifiers.

CONFLICT OF INTEREST

The authors have no conflict of interest to disclose.

ORCID

Michael Melek https://orcid.org/0000-0001-8624-4820
Ahmed Khattab https://orcid.org/0000-0002-3425-9833

REFERENCES

1. Daugman, J.G.: High confidence visual recognition of persons by a test of statistical independence. IEEE Trans. Pattern. Anal. Mach. Intell. 15(11), 1148–1161 (1993)
2. Daugman, J.: How iris recognition works. In: AI. Bovik, (Ed.), The Essential Guide to Image Processing, pp. 715–739. Austin Texas: Elsevier (2009)
3. Rathgeb, C., Busch, C.: Iris and Periocular Biometric Recognition. Institution of Engineering and Technology. UK (2017)
4. Jolliffe, I.: Principal component analysis. Wiley Online Library. New Jersy (2002)
5. Turk, M., Pentland, A.: Eigenfaces for recognition. J. Cognit. Neurosci. 3(1), 71–86 (1991)
6. Belhumeur, P.N., Hespanha, J.P., Kriegman, D.J.: Eigenfaces vs. fisherfaces: recognition using class specific linear projection. IEEE Trans. Pattern Anal. Mach. Intell. 19(7), 711–720 (1997)
7. He, X., Niyogi, P.: Locality preserving projections. NIPS (News Physiol Sci.) 16, 153–160 (2003)
8. Wright, J., et al.: Robust face recognition via sparse representation. IEEE Trans. Pattern Anal. Mach. Intell. 31(2), 210–227 (2009)
9. Pillai, J.K., et al.: Secure and robust iris recognition using random projections and sparse representations. IEEE Trans. Pattern Anal. Mach. Intell. 33(9), 1877–1893 (2011)
10. Canddès, E.J., et al.: Compressive sampling. In: Proceedings of the International Congress of Mathematicians, vol. 3, pp. 1433–1452. Madrid (2006)
11. Donoho, D.L.: Compressed sensing. IEEE Trans. Inf. Theory. 52(4), 1289–1306. (2006)
12. Tropp, J.A., Gilbert, A.C.: Signal recovery from random measurements via orthogonal matching pursuit. IEEE Trans. Inf. Theory, 53(12), 4655–4666 (2007)
13. Abdel.Sayed, M.M., et al.: Adaptive reduced-set matching pursuit for compressed sensing recovery. In: 2016 IEEE International Conference on Image processing (ICIP). Phoenix, AZ (2016)
14. Bhateja, A.K., et al.: Iris recognition based on sparse representation and k-nearest subspace with genetic algorithm. Pattern Recogn. Lett. 73, 13–18 (2016)
15. Cui, J., et al.: An iris image synthesis method based on PCA and super-resolution. In: Proceedings of the 17th International Conference on Pattern Recognition, vol. 4, 471–474. IEEE, Cambridge, UK (2004)
16. Te Chu, C., Chen, C.H.: High performance iris recognition based on LDA and LPCC. In: 17th IEEE International Conference on Tools with Artificial Intelligence (ICTAI05). pp. 5. IEEE, Hong Kong, China (2005)
17. Chen, W.S., et al.: Iris recognition using 2d-LDA+ 2d-PCA. In: 2009 IEEE international conference on Acoustics, Speech and Signal Processing, pp. 869–872. IEEE, Taipei, Taiwan (2009)
18. Huang, Y.P., Luo, S.W., Chen, E.Y.: An efficient iris recognition system. In: Proceedings of the International Conference on Machine Learning and Cybernetics, vol. 1, pp. 450–454. IEEE, Beijing, China (2002)
19. Huo, G., et al.: Multi-source heterogeneous iris recognition using locality preserving projection. In: Chinese Conference on Biometric Recognition, pp. 304–311. Springer, Zhuzhou, China (2019)

20. Kumar, N., Rawat, M.: Rp-lpp: a random permutation based locality preserving projection for cancellable biometric recognition. Multimed. Tool. Appl. 79(3), 2363–2381 (2020)
21. Shashi Kumar, D.R., et al.: PCA based iris recognition using dwt. Int. J. Comp. Tech .Appl. 2(4), 884–893 (2011)
22. Minaee, S., Abdolrashidi, A., Wang, Y.: Iris recognition using scattering transform and textural features. In: 2015 IEEE signal processing and signal processing education workshop (SP/SPE). pp. 37–42. IEEE, Salt Lake City, UT (2015)
23. Melek, M., Khattab, A., Abu.Elyazeed, M.F.: Fast matching pursuit for sparse representation-based face recognition. IET Image Process. 12(7), 1807–1814 (2018)
24. Minaee, S., et al.: Biometric recognition using deep learning: a survey, arXiv preprint arXiv:191200271 (2019)
25. Gangwar, A., Joshi, A.: DeepIrisNet: Deep iris representation with applications in iris recognition and cross-sensor iris recognition. In: 2016 IEEE international conference on image processing (ICIP), pp. 2301–2305.IEEE, Phoenix, AZ (2016)
26. Nguyen, K., et al.: Iris recognition with off-the-shelf CNN features: a deep learning perspective. IEEE Access. 6, 18848–18855 (2017)
27. Zhao, T., et al.: A deep learning iris recognition method based on capsule network architecture, IEEE Access. 7, 49691–49701 (2019)
28. Alaslani, M.G., Elrefaei, L.A.: Convolutional neural network based feature extraction for iris recognition. Int. J. Comput. Sci. Inf. Technol. 10(2), 65–78 (2018)
29. Minaee, S., Abdolrashidiy, A., Wang, Y.: An experimental study of deep convolutional features for iris recognition. In: 2016 IEEE signal processing in medicine and biology symposium (SPMB). pp. 1–6. IEEE (2016)
30. Minaee, S., Abdolrashidi, A.: DeepIris: Iris recognition using a deep learning approach (2019)
31. Menon, H., Mukherjee, A.: Iris biometrics using deep convolutional networks. In: 2018 IEEE International Instrumentation and Measurement Technology Conference (I2MTC), pp. 1–5. IEEE, Houston, TX (2018)
32. Arsalan, M., et al.: Deep learning-based iris segmentation for iris recognition in visible light environment. Symmetry. 9(11), 263 (2017)
33. Duda, R.O., Hart, P.E.: Use of the hough transformation to detect lines and curves in pictures. Commun. ACM. 15(1), 11–15 (1972)
34. Shen, L., Bai, L.: A review on gabor wavelets for face recognition. Pattern Anal. Appl. 9(2–3), 273–292 (2006)
35. Gabor, D.: Theory of communication. part 1: the analysis of information. J. Inst. Electr. Eng. 3. 93(26), 429–441 (1946)
36. Daugman, J.G.: Uncertainty relation for resolution in space, spatial frequency, and orientation optimised by two-dimensional visual cortical filters. JOSA A. 2(7), 1160–1169 (1985)
37. Liu, C., Wechsler, H.: Gabor feature based classification using the enhanced Fisher linear discriminant model for face recognition. IEEE Trans Image Process. 11(4), 467–476 (2002)
38. Sun, B., et al.: Comparative study of compressive classification-based approaches for face recognition. In: 2016 IEEE 11th Conference on Industrial Electronics and Applications (ICIEA). pp. 689–693. IEEE (2016)
39. He, X., et al.: Face recognition using laplacianfaces. IEEE Trans. Pattern Anal. Mach. Intell. 27, (3), pp. 328–340 2005
40. Belkin, M., Niyogi, P.: Laplacian eigenmaps and spectral techniques for embedding and clustering. NIPS (News Physiol Sci). 14, 585–591 (2001)
41. Eldar, Y.C., Kutyniok, G.: Compressed sensing: theory and applications. Cambridge University Press, UK (2012)
42. Abdel.Sayed, M.M., et al.: Reduced-set matching pursuit approach for efficient compressed sensing signal reconstruction. J. Adv. Res. 7(6), 851–861 (2016)
43. CASIA Iris Database: Version 1.0. Chinese Academy of Sciences Institute of Automation (CASIA). http://biometrics.idealtest.org/
44. IIT Delhi iris database version 1.0. http://web.iitd.ac.in/~biometrics/Database_Iris.htm
45. Kohavi, R., et al.: A study of cross-validation and bootstrap for accuracy estimation and model selection. In: International Joint Conferences on Artificial Intelligence, vol. 14, pp. 1137–1145. Stanford (1995)

How to cite this article: Melek M, Abu-Elyazeed MF, Khattab A. Efficient high-speed framework for sparse representation-based iris recognition. *IET Biome.* 2021;10:304–314. https://doi.org/10.1049/bme2.12022